sustainability

MDPI

Article

Optimizing Performance of a Solar Flat Plate Collector for Sustainable Operation Using Box–Behnken Design (BBD)

Ramesh Chitharaj [1,*], Hariprasad Perumal [1], Mohammed Almeshaal [2] and P. Manoj Kumar [3,*]

[1] Department of Mechanical Engineering, KIT-Kalaignarkarunanidhi Institute of Technology, Coimbatore 641402, Tamil Nadu, India
[2] Department of Mechanical Engineering, College of Engineering, Imam Mohammad Ibn Saud Islamic University, Riyadh 11432, Saudi Arabia
[3] Department of Mechanical Engineering, KPR Institute of Engineering and Technology, Coimbatore 641407, Tamil Nadu, India
* Correspondence: crameshphd@gmail.com (R.C.); manojkumar.p@kpriet.ac.in (P.M.K.)

Abstract: This study investigated the performance optimization of nickel-cobalt (Ni-Co)-coated absorber panels in solar flat plate collectors (SFPCs) using response surface methodology for sustainable operation and optimized performance. Ni-Co coatings, applied through an electroplating process, represent a novel approach by offering superior thermal conductivity, durability, and environmental benefits compared to conventional black chrome coatings, addressing critical concerns related to ecological impact and long-term reliability. Experiments were conducted to evaluate the thermal efficiency of Ni-Co-coated panels with and without reflectors under varying flow rates, collector angles, and reflector angles. The thermal efficiency was calculated based on the inlet and outlet water temperatures, solar radiation intensity, and panel area. The results showed that the SFPC achieved average efficiencies of 50.9% without reflectors and 59.0% with reflectors, demonstrating the effectiveness of the coatings in enhancing solar energy absorption and heat transfer. A validated quadratic regression model (R^2 = 0.9941) predicted efficiency based on the process variables, revealing significant individual and interaction effects. Optimization using the Box–Behnken design identified the optimal parameter settings for maximum efficiency: a flow rate of 1.32 L/min, collector angle of 46.91°, and reflector angle of 42.34°, yielding a predicted efficiency of 79.2%. These findings highlight the potential of Ni-Co coatings and reflectors for enhancing SFPC performance and provide valuable insights into the sustainable operation of solar thermal systems. Furthermore, the introduction of Ni-Co coatings offers a sustainable alternative to black chrome, reducing environmental risks while enhancing efficiency, thereby contributing to the advancement of renewable energy technologies.

Keywords: Ni-Co coatings; solar flat plate collectors (SFPCs); thermal efficiency; response surface methodology; optimization; black chrome coatings

check for updates

Academic Editor: Firoz Alam

Received: 30 November 2024
Revised: 6 January 2025
Accepted: 7 January 2025
Published: 9 January 2025

Citation: Chitharaj, R.; Perumal, H.; Almeshaal, M.; Manoj Kumar, P. Optimizing Performance of a Solar Flat Plate Collector for Sustainable Operation Using Box–Behnken Design (BBD). *Sustainability* **2025**, *17*, 461. https://doi.org/10.3390/su17020461

Copyright: © 2025 by the authors. Licensee MDPI, Basel, Switzerland. This article is an open access article distributed under the terms and conditions of the Creative Commons Attribution (CC BY) license (https://creativecommons.org/licenses/by/4.0/).

1. Introduction

Solar energy, an inexhaustible and clean source of energy, has immense potential to meet the growing energy demands of modern societies while mitigating the environmental impacts associated with fossil fuel usage [1–3]. Over the last few decades, harnessing solar energy using various technologies has become a key area of research and development [4,5]. Recent studies have demonstrated the significant sustainability benefits of solar energy systems. For example, solar collectors can reduce greenhouse gas emissions by up to 70%,

while achieving energy efficiencies exceeding 85% [6]. Similarly, solar drying systems have been shown to completely eliminate CO_2 emissions compared to conventional electric convective dryers, which emit 294–410 kg CO_2 per kWh [7]. These findings underscore the potential of solar energy technologies to contribute to environmental sustainability and cost efficiency. Among these technologies, solar thermal systems, particularly solar flat plate collectors (SFPCs), are widely recognized for their versatility, reliability, and adaptability to diverse applications ranging from water heating to industrial processes [8–11]. However, one of the primary challenges in this field is to improve the efficiency of these collectors to make them a more viable and competitive option than conventional energy sources [12–14]. The ability of SFPCs to effectively capture, absorb, and retain solar radiation is directly related to the materials and design characteristics of their absorber plates. Enhancements in this area can significantly improve the thermal performance of solar collectors, thus driving advancements in the practical applications of solar thermal technology.

One of the key strategies for enhancing the thermal efficiency of SFPCs is the use of specialized coatings on absorber panels. These coatings are designed to improve the selective absorption of solar radiation while minimizing thermal losses due to radiation. Typically, absorber plates are treated with selective coatings that exhibit high absorptance and low emittance, which help convert a greater portion of the incident solar energy into usable thermal energy. Traditional coating materials, such as black chrome (BC) [15–22], have been extensively employed owing to their favorable properties, including high thermal stability and robust absorption–emission characteristics. However, despite the advantages of BC coatings, they have certain limitations, including environmental concerns related to the use of Cr, which is a hazardous material, and performance limitations under specific operating conditions. These challenges have spurred interest in alternative coating materials that can offer similar or even superior thermal performance while addressing the environmental and durability concerns of conventional coatings.

In this study, nickel-cobalt (Ni-Co) coatings emerged as a promising alternative to black chrome for solar absorber panels. Ni-Co coatings possess several advantageous properties that make them suitable for solar thermal applications, including high thermal conductivity, good corrosion resistance, and the ability to be engineered for selective absorption–emission characteristics [23–29]. These coatings can be deposited through electroplating, a process that allows control over the composition, thickness, and surface morphology of the coating layer. The Ni-Co alloy composition can be adjusted to optimize its optical and thermal properties, enabling its tailored application in solar collectors. Furthermore, the use of Ni-Co coatings can mitigate some of the environmental concerns associated with chromium-based coatings, as Ni and Co are generally considered less hazardous when handled and disposed of appropriately. Despite these advantages, research on Ni-Co coatings for solar thermal applications, particularly SFPCs, remains limited, and there is a need to explore their thermal efficiency under various operational conditions to fully understand their potential.

Although the potential of Ni-Co coatings as a replacement for BC coatings is increasingly recognized, there are significant gaps in the literature concerning their performance optimization in SFPCs. Existing studies have largely focused on the development and characterization of Ni-Co coatings without extensive investigation of their practical application under realistic operating conditions in solar collectors. For instance, parameters such as flow rate, collector angle, and the use of reflectors are known to significantly influence the thermal performance of SFPCs; however, their effects on Ni-Co-coated absorber panels remain under-explored. BC coatings have traditionally been favored owing to their established thermal efficiency profiles under various environmental conditions; however, their drawbacks have created an opportunity for new materials, such as Ni-Co, to be tested as

viable alternatives. Furthermore, the effectiveness of these coatings in conjunction with reflectors, which are often used to increase solar radiation on the collector surface, has not been adequately investigated. Reflectors can significantly enhance the efficiency of solar collectors by redirecting additional sunlight to the absorber panel, thereby maximizing the absorbed solar energy. The combination of Ni-Co coatings and reflectors could potentially offer a synergistic improvement in thermal efficiency; however, this possibility has received limited attention in the research community.

The choice to focus on Ni-Co coatings rather than traditional BC coatings is driven by both environmental and performance considerations. The production and disposal of chromium-based materials, such as BC, present substantial ecological risks owing to the toxicity and carcinogenic nature of chromium. In contrast, Ni-Co coatings, when properly managed, represent a comparatively safer alternative with reduced environmental impact. Moreover, Ni-Co coatings provide additional flexibility in terms of tuning their thermal and optical properties through compositional adjustments, which can be advantageous for optimizing coatings for specific applications and conditions. However, to date, there has been insufficient research aimed at optimizing the performance of Ni-Co coatings for SFPCs. Addressing this knowledge gap is essential for establishing Ni-Co coatings as viable and sustainable alternatives to BC in solar thermal applications.

The objective of this study was to investigate the performance of Ni-Co-coated absorber panels in SFPCs, with a particular focus on optimizing the thermal efficiency under variable operating conditions. Specifically, this study examines the impact of key process variables, including the flow rate, collector angle, and reflector angle, on the thermal performance of Ni-Co-coated panels. By conducting a systematic analysis of these variables, this study seeks to provide insights into the conditions under which Ni-Co coatings can achieve maximum efficiency in solar thermal applications. Additionally, this study explored the effect of using reflectors in conjunction with Ni-Co-coated panels to assess whether this combination can yield enhanced thermal performance compared to Ni-Co coatings alone.

To achieve these objectives, this research methodology incorporates both experimental and analytical approaches to evaluate the thermal efficiency of Ni-Co-coated panels under controlled conditions. Experimental testing involved varying the flow rate of the working fluid within the collector, adjusting the angle of the collector to optimize solar radiation absorption, and modifying the reflector angle to maximize the incident solar energy. The results were analyzed to identify the optimal configurations for enhancing the thermal efficiency of the SFPC system. Furthermore, by comparing the performance of Ni-Co-coated panels with and without reflectors, this study aimed to determine the extent to which reflectors contribute to the efficiency gains achievable with Ni-Co coatings. In addition, this study emphasizes the sustainability of solar energy systems by focusing on Ni-Co-coated SFPCs as a viable alternative to conventional heating systems that rely on fossil fuels and emit significant GHGs. This research highlights the environmental benefits of reducing carbon emissions while optimizing the thermal efficiency of solar systems, thereby contributing to global efforts toward sustainable energy solutions.

2. Materials and Methods

2.1. Experimental Setup

The experimental setup for this study was designed around a Solar Flat Plate Collector (SFPC) incorporating Ni-Co-coated absorber panels, as shown in Figure 1. The SFPC apparatus includes essential components, such as an absorber panel, glazing, insulation, and tubing. The setup was aimed at evaluating the thermal efficiency of the Ni-Co-coated panels, with and without reflectors, under controlled conditions. The Ni-Co coating on the absorber panels was applied using an electroplating technique designed to yield a layer

thickness of approximately 18.6 µm. This coating thickness was selected based on previous studies, indicating an optimal balance between thermal efficiency and material stability. The process began with surface preparation, where the copper plate was polished and degreased using a sodium hydroxide (NaOH) solution to remove any contaminants. The surface was activated using hydrochloric acid (HCl). Subsequently, the electroplating bath, comprising a nickel-cobalt electrolyte solution, facilitated the coating deposition. The Ni-Co coating provided high absorptivity for solar radiation while maintaining the durability required for long-term solar thermal applications.

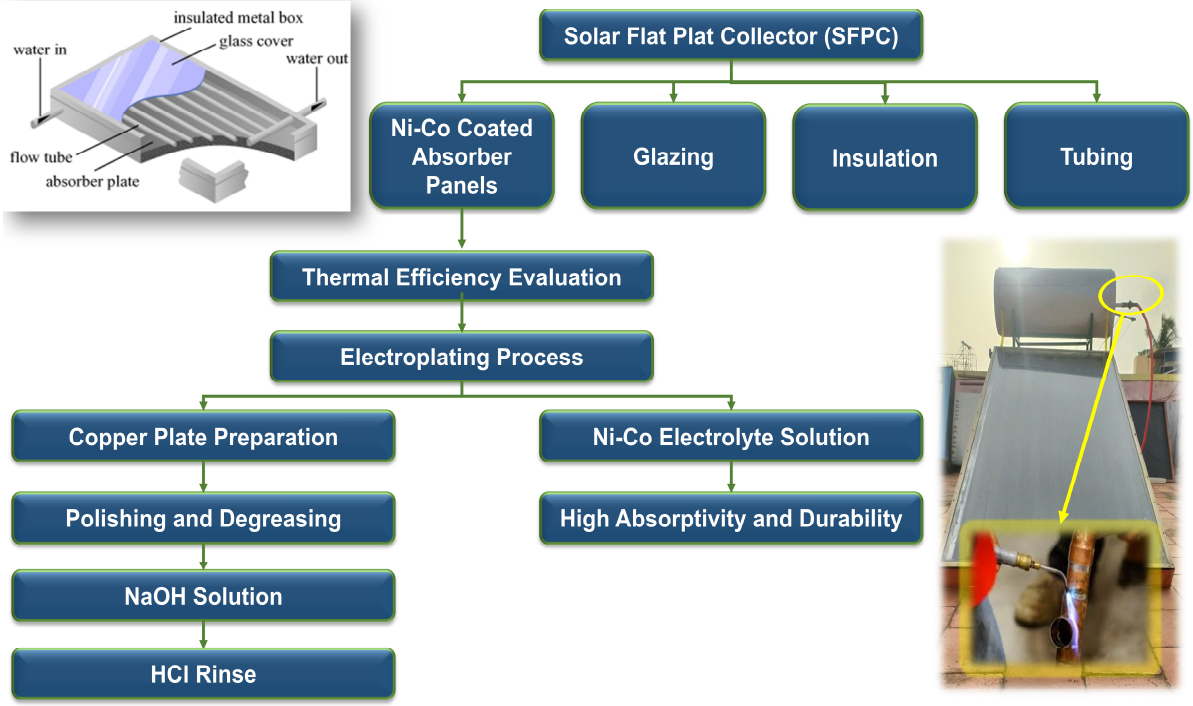


Figure 1. SFPC with Ni-Co-coated absorber panel.

2.2. Data Collection Procedure

The experiments were conducted over the course of the second week of April 2024 under optimal weather conditions and sunny skies with no cloud cover to ensure consistent solar radiation and reduce variability due to atmospheric factors. Data were collected daily from 08:00 to 06:00 (GMT +5.30), covering the entire period of maximum solar exposure. Before beginning each day's experiment, the Solar Flat Plate Collector (SFPC), including the glazing and absorber panel, was thoroughly cleaned and inspected to ensure optimal operation and minimize discrepancies in the collected data. At the start of the experiment, the reflectors were set to a flat position (0° relative to the SFPC), and the collector angle was fixed at 45° relative to the ground to standardize the initial setup. The water flow rate was set to 1 L per minute (L/min) using a flow meter installed at the outlet header. The flow rate was established and stabilized 30 min prior to the start of data collection to ensure consistent conditions throughout the experiment. At 08:00 a.m., data recording began. The inlet (T1) and outlet (T2) water temperatures were measured along with the incident solar radiation (SR) on the SFPC. These measurements formed the basis of the thermal efficiency calculations. The same set of data (T1, T2, and SR) was collected hourly from 08:00 a.m. to 06:00 p.m. to capture the daily variation in solar radiation and its effects on the thermal performance of the SFPC. These steps were repeated for three consecutive days. The average data from these three days were used in subsequent analyses to enhance the reliability and accuracy of the output, thus minimizing the influence of minor fluctuations

in environmental conditions. Following the initial data collection phase, the reflectors were adjusted to a 45° angle relative to the SFPC to investigate their effects on thermal efficiency. With the reflector angle modified, steps 2–5 were repeated over the next three days to gather comparative data.

2.3. Thermal Efficiency Calculation

The recorded experimental data were analyzed to determine the thermal efficiency (η) of the solar flat plate collector (SFPC) over time. According to various studies [30–36], the thermal efficiency of the solar water heating (SWH) system was calculated using the following formula (Equation (1)):

$$\eta = \frac{m \times C_p \times (T_2 - T_1)}{A \times G} \quad (1)$$

where m represents the mass flow rate of water (kg/s).

C_p: specific heat capacity of water at constant pressure (J/kg·K).

For water, Cp was approximately 4186 J/kg·K at room temperature.

T_1—inlet temperature of water (°C).

T_2—outlet temperature of water (°C).

A—the effective area of the absorber panel (m^2).

G—intensity of solar radiation (W/m^2).

3. Single Objective Optimization of Process Variables

3.1. Range of Parameters

The selection of the flow rate, collector angle, and reflector angle was based on their critical influence on the thermal performance and efficiency of solar flat plate collectors. The flow rate was varied to optimize heat transfer and thermal utilization, with previous studies reporting optimal results at higher flow rates such as 3.5 kg/min, achieving peak efficiencies of 23% [37]. The collector angle was adjusted to capture the maximum solar irradiance, ensuring optimal alignment with the sun's trajectory, as demonstrated in similar experimental setups [38]. Reflector angles were chosen to enhance the concentration of solar energy on the absorber surface, a strategy proven effective in improving output temperatures and system efficiency. These ranges were determined through iterative design and validated against the established literature. From these inputs, the control variables and their levels were set as listed in Table 1. The experimental conditions were systematically varied according to the 17-run Design of Experiments (DOE) established in this study. For each run, a specific combination of the flow rate, collector angle, and reflector angle (Table 2) was implemented. Data for T1, T2, and SR were recorded hourly throughout the day for each run for a total of 17 days of data collection to complete the DOE sequence.

Table 1. Control variables and their levels.

S. No.	Variables	Units	Levels		
			Low (−1)	Medium (0)	High (+1)
1	The volume flow rate of water (V_0)	L/min	0.5	1.5	2.5
2	Collector inclination (θ)	Degree	30	45	60
3	Reflector inclination (α)	Degree	30	45	60

Table 2. Matrix of process variables.

S. No.	Flow Rate (V_0)	Collector Angle (θ)	Reflector Angle (α)
	L/min	Degree	Degree
1	1.5	45	45
2	2.5	45	30
3	0.5	30	45
4	0.5	45	30
5	1.5	45	45
6	1.5	45	45
7	2.5	45	60
8	1.5	30	30
9	0.5	45	60
10	2.5	30	45
11	1.5	45	45
12	1.5	60	60
13	1.5	45	45
14	1.5	60	30
15	0.5	60	45
16	1.5	30	60
17	2.5	60	45

3.2. Statistical Data Analysis

Following data collection, statistical analysis was conducted to develop a regression model (Figure 2) that describes the relationship between the process variables and thermal efficiency. This model, based on the response surface methodology (RSM), serves as the foundation for optimization. The regression model can take different forms, namely, linear, quadratic, or higher-order, based on the relationships observed. The suitability of each model was evaluated by assessing the data fit and interaction significance. The Box–Behnken Design (BBD) was utilized for the experimental design and optimization, as shown in Figure 3.

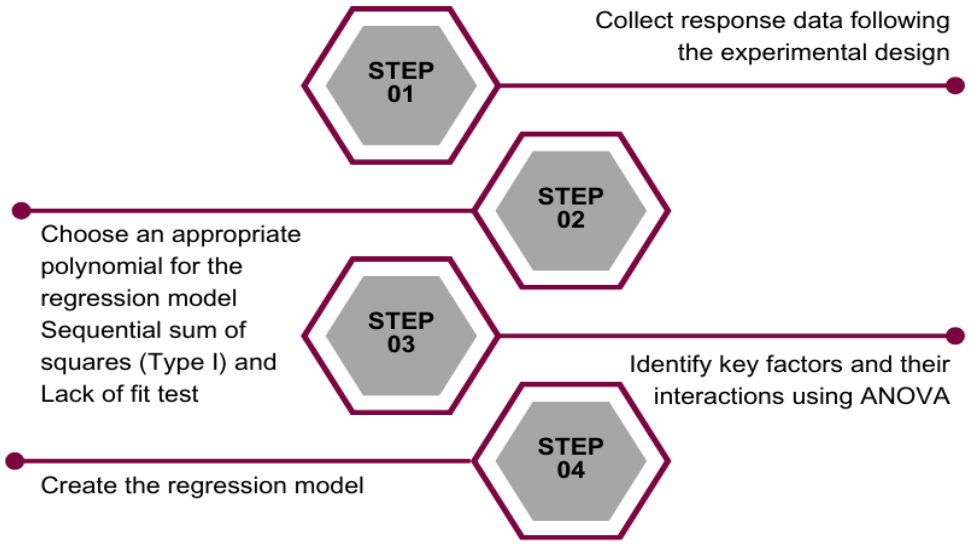


Figure 2. Development of regression model.

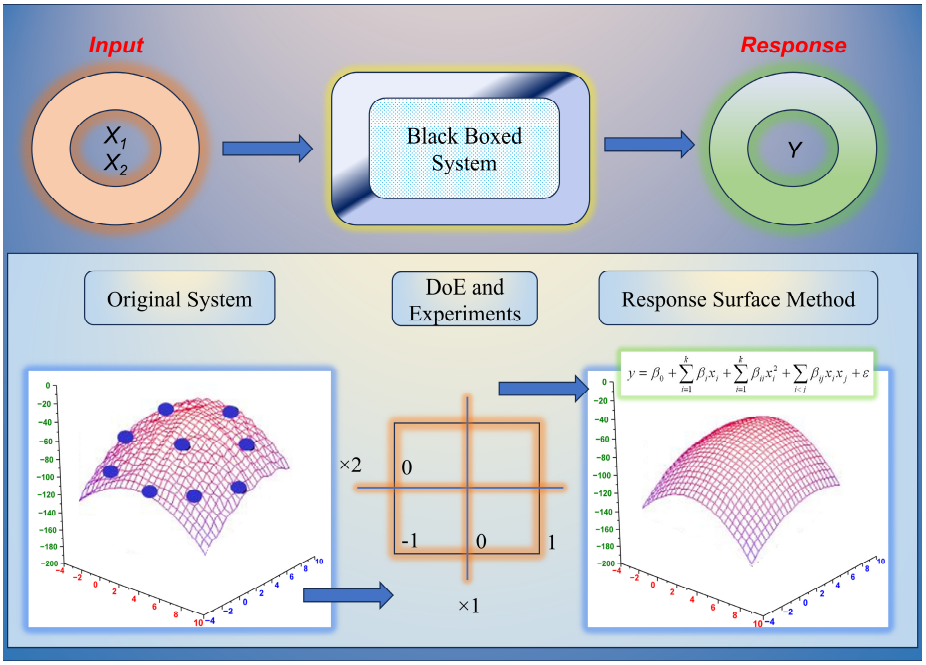


Figure 3. Box–Behnken design (BBD).

The Box–Behnken Design (BBD) using Design Expert software (version 7.0) was selected over other designs, such as the Central Composite Design (CCD), due to its superior efficiency in requiring fewer experimental runs (15 for three factors, compared to 20 or more for CCD). This efficiency minimizes experimental time and resource use while maintaining robust predictive accuracy. In addition, BBD avoids extreme factor combinations that can destabilize the system, thereby ensuring that the process variables remain within safe and practical operating ranges. The design is particularly well suited for optimizing thermal and solar energy systems, where interaction and quadratic effects are critical for understanding system behavior. Its spherical design space and reduced sensitivity to measurement errors further enhance its suitability for this study. After that, the statistical models were validated using analysis of variance (ANOVA), and the regression coefficients were used to predict the optimal operating conditions. The adequacy of the quadratic model was evaluated based on the coefficient of determination (R^2), adjusted R^2, and predicted R^2 values, which ensured the reliability of the design for optimization.

3.3. Sequential Model Sum of Square (SMSS)

Sequential model sum-of-squares analysis compares models with increasing complexities. For example, it tests whether adding quadratic terms improves the model fit. Only models with terms that met the significance threshold ($p < 0.1$) were retained.

3.4. Lack of Fit (LF)

The lack of fit indicates how well the model fits the experimental data. A model with a significant lack of fit cannot reliably predict outcomes and is therefore unsuitable. This study aimed for an insignificant lack of fit, indicating that the model accurately represented the collected data.

3.5. Model Summary Statistics

The model summary includes key metrics, such as adjusted R-squared, predicted R-squared, and Prediction Error Sum of Squares (PRESS). An ideal model will have R-squared values close to 1, low PRESS, and minimal standard deviation.

3.6. Analysis of Variance (ANOVA)

ANOVA was used to determine the statistical significance of model terms and interactions. Key points include:

- **Model significance:** Confirmed if prob > F value is below 0.05, indicating that the term is influential.
- **Predicted vs. adjusted R-squared:** A difference of less than 0.2 suggests good model reliability.
- **Adequate precision:** This metric (recommended as >4) was used to assess the signal-to-noise ratio.

3.7. Statistics Optimization by Response Surface Methodology (RSM)

The model developed in the previous step was used to identify the optimal settings for the SFPC parameters. The optimization was aimed at maximizing the thermal efficiency by adjusting the flow rate, collector angle, and reflector angle within predefined constraints. This analysis was performed using the desirability function approach in Design Expert 13.0, providing a practical balance between model accuracy and parameter constraints.

4. Results and Discussions

4.1. Performance of Ni-Co-Coated Absorber Panel

The thermal performance of the Ni-Co-coated absorber panel without reflectors was evaluated by recording the ambient temperature, exit water temperature, incident solar radiation, and efficiency over the course of the day from 08:00 a.m. to 06:00 p.m. Figure 4 illustrates the hourly variations in these parameters. The data provide key insights into the behavior and efficiency of the Ni-Co coating in solar energy absorption and heat transfer under direct sunlight without additional reflection.

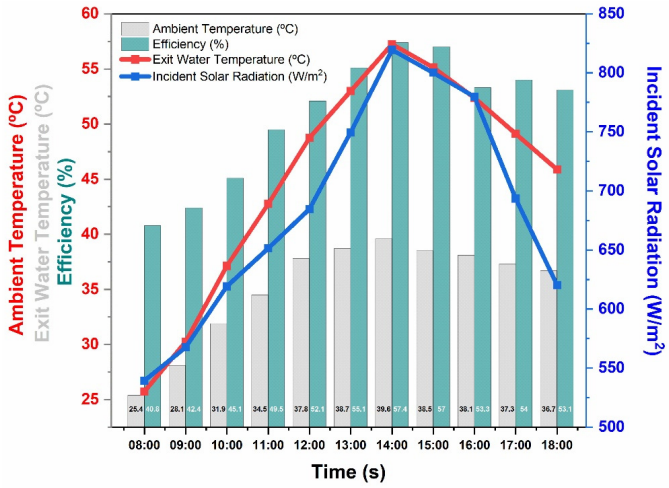


Figure 4. Performance of Ni-Co-coated absorber panel.

4.1.1. Performance of Ni-Co Panel Without Reflector (Time vs. Exit Water Temperature)

The exit water temperature gradually increased throughout the morning hours, peaking in the early afternoon at 60.3 °C at 2:00 p.m., before gradually decreasing as the day progressed and solar radiation decreased. This trend is consistent with studies that highlight the diurnal variation in solar energy absorption, which generally follows the solar irradiance pattern, peaking around solar noon owing to the maximum solar incidence. From an initial morning temperature of 35.1 °C at 08:00 a.m., the temperature of the water exiting the panel rose steadily as solar radiation intensified, demonstrating the effectiveness of Ni-Co coatings in capturing and retaining heat within the absorber plate. The gradual

increase in the exit water temperature aligns with the literature findings, which reported that selective coatings, such as Ni-Co, are advantageous in enhancing the thermal performance owing to their high absorptivity and relatively low emissivity compared to uncoated surfaces. The peak temperature recorded in this study, 60.3 °C, indicates the capacity of the Ni-Co coating to absorb substantial heat, even without reflectors to augment solar input.

4.1.2. Performance of Ni-Co Panel Without Reflector (Time vs. Incident Solar Radiation)

The incident solar radiation, which peaked at 819.4 W/m^2 at 2:00 p.m., closely correlated with the recorded exit water temperatures, as both reached their maximum values around the same time. This relationship is typical in solar thermal applications because the amount of absorbed solar radiation is directly proportional to the heat transfer achieved by the system. The incident radiation began at 539.4 W/m^2 in the morning and progressively increased, tracking closely with the solar altitude angle until peaking in the early afternoon. Subsequently, it declined as the sun's position shifted toward the horizon. The observed pattern of solar radiation throughout the day, along with the corresponding variations in the exit water temperature, supports the concept of selective coatings that enhance the solar absorption efficiency of the collector. As noted in the literature, selective coatings such as Ni-Co are designed to maximize the absorption of shortwave solar radiation while minimizing thermal losses through radiation. This characteristic is evident in the performance of the Ni-Co panel, as it maintained high exit temperatures even when solar radiation began to decrease in the late afternoon.

4.1.3. Performance of Ni-Co Panel Without Reflector (Time vs. Efficiency)

The efficiency of the Ni-Co coated panel exhibited a gradual increase from 40.8% at 08:00 a.m. to a maximum of 57.4% at 2:00 p.m., and then gradually declined to 53.1% at 6:00 p.m. This efficiency pattern reflects the combined effect of solar radiation intensity, ambient temperature, and properties of the Ni-Co coating. The solar collector efficiency depends on factors such as the optical characteristics of the collector, incident solar radiation, and thermal losses. In the present study, the efficiency values were highest during peak solar hours, suggesting that the Ni-Co coating was effective in capturing and converting solar radiation into heat energy. However, the observed decline in efficiency during the late afternoon, even when the exit water temperature remained relatively high, suggests a diminishing effect of solar input compared to the increased thermal losses as the ambient temperature starts to decrease.

The average efficiency during the day was 50.9%, which aligns with the findings of previous studies [35,39] on selective coatings for solar thermal applications. For instance, Kumar et al. [39] reported similar efficiency values for Ni-based coatings, demonstrating their potential for applications that require moderate to high thermal efficiency. Compared to conventional coatings, such as black chrome, Ni-Co coatings offer superior environmental benefits and corrosion resistance, making them a more sustainable and economically feasible option. The electroplating process for Ni-Co coatings eliminates hazardous chemicals, reduces production costs and environmental risks, and enhances thermal stability and durability [40]. These advantages extend the lifecycle of solar collectors, minimize operational costs, and, when combined with their higher efficiency, position Ni-Co coatings as a transformative solution for solar thermal systems. Furthermore, Ni-Co coatings, compared to other eco-friendly alternatives such as sol-gel coatings and selective black paints, demonstrate a lower environmental impact on a lifecycle basis. Their energy-efficient production process, avoidance of hazardous materials, and superior recyclability make them a sustainable choice for solar collector systems. Additionally, their enhanced durability and

high thermal efficiency reduce material usage and associated lifecycle emissions, further contributing to their environmental benefits.

4.1.4. Comparative Analysis with Uncoated or Conventionally Coated Panels

Compared with uncoated or conventionally coated panels, the Ni-Co coating demonstrates competitive performance in terms of exit water temperature and efficiency without the use of reflectors. Although adding reflectors would likely enhance the thermal efficiency by increasing the incident solar radiation, the performance observed without reflectors underscores the capability of the Ni-Co coatings to absorb and retain heat effectively. The ability of Ni-Co coatings to achieve average efficiencies above 50% without reflectors makes them suitable for applications in climates with high solar irradiance.

4.2. Performance of Ni-Co-Coated Absorber Panel with Reflectors

The use of reflectors in conjunction with Ni-Co-coated absorber panels enhances the incident solar radiation and subsequently improves the thermal performance of a solar flat plate collector (SFPC). In this section, we analyze the results of the Ni-Co-coated panel with reflectors by examining the variations in the exit water temperature, solar radiation, and efficiency throughout the day. The data presented in Figure 5 indicate significant improvements in the thermal efficiency and exit water temperature when reflectors are employed, showing the potential of reflectors in optimizing the performance of Ni-Co coatings in solar thermal applications.

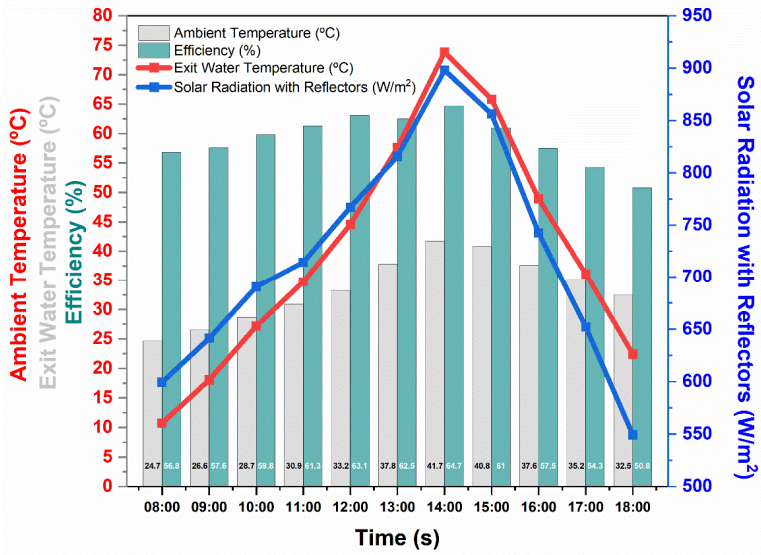


Figure 5. Performance of Ni-Co-coated absorber panel with reflectors.

4.2.1. Performance of Ni-Co Panel with Reflector (Time vs. Exit Water Temperature)

The exit water temperature in the Ni-Co-coated panel with reflectors showed a substantial increase compared with the configuration without reflectors, as shown in Figure 5. Starting from an initial temperature of 39.7 °C at 08:00 a.m., the exit water temperature reached its peak at 67.3 °C at 2:00 p.m., following the peak of the incident solar radiation. This increase was approximately 7 °C higher than the peak temperature observed in the absence of reflectors, highlighting the impact of the additional solar radiation reflected on the absorber surface. The temperature profile indicates that the reflectors effectively increased the thermal absorption capacity of the Ni-Co-coated panel by concentrating more solar energy on the surface. This finding aligns with those of previous studies [36], which demonstrated that solar reflectors can significantly enhance the solar collector performance by increasing the solar flux received by the absorber. Additionally, the maximum

outlet water temperature achieved with Ni-Co-coated plates and reflectors was 67.3 °C, which exceeds the range of 50–60 °C reported in systems using selective black paint coatings [38]. This demonstrates the potential of Ni-Co coatings to meet the thermal demands of high-temperature applications, such as industrial drying and sterilization processes. The elevated exit water temperature achieved with the reflectors confirms the suitability of the Ni-Co coatings for high-efficiency solar thermal applications when supplemented with additional reflectors.

4.2.2. Performance of Ni-Co Panel with Reflector (Time vs. Incident Solar Radiation)

The incident solar radiation with reflectors peaked at 898.1 W/m^2 at 2:00 p.m., which is significantly higher than the maximum radiation recorded without reflectors. The addition of reflectors effectively enhanced solar radiation exposure throughout the day, with an average daily solar radiation of 720.6 W/m^2, compared to 684.1 W/m^2 without reflectors. This increase of approximately 36.5 W/m^2 translates into a greater thermal energy input to the SFPC, which, as observed, results in higher exit water temperatures and improved efficiency. These results confirm the beneficial impact of reflectors on solar energy collection because enhanced solar radiation leads to higher thermal gains within the absorber panel. The present data demonstrate that the Ni-Co-coated panel responds effectively to this increased solar input, making it an excellent candidate for configurations that include reflectors.

4.2.3. Performance of Ni-Co Panel with Reflector (Time vs. Efficiency)

The thermal efficiency of the Ni-Co-coated panel with reflectors increased throughout the day, reaching a maximum of 64.7% at 2:00 p.m. The efficiency values gradually increased from 56.8% in the morning (08:00 a.m.), and an average efficiency of 59.0% was achieved for the entire day. The efficiency pattern closely follows the incident solar radiation trend, peaking when the solar radiation is the highest and declining as the radiation decreases toward the evening. This average efficiency of 59.0% with reflectors represents an improvement of approximately 8% compared to the average efficiency without reflectors (50.9%). The increased efficiency demonstrates the effectiveness of the reflectors in improving the thermal performance of the Ni-Co coating, as additional solar radiation is directed onto the absorber panel, thereby increasing the overall energy captured and transferred to the working fluid. The improved efficiency observed with reflectors underscores the potential of integrating reflector-based designs with Ni-Co coatings to maximize the solar thermal output. Although emissivity remains a concern for Ni-Co coatings, as noted in previous studies [41], the efficiency boost provided by reflectors mitigates some of these thermal losses by increasing the overall thermal input.

4.2.4. Comparative Analysis Against Absorber Panel Without Reflectors

The performance analysis of the Ni-Co-coated absorber panel with reflectors revealed a substantial improvement in the exit water temperature, incident solar radiation, and thermal efficiency. The reflector setup provided an increase in the incident solar radiation and exit water temperature, with a day-average efficiency improvement of 8% compared with the setup without reflectors. This aligns with findings by Ullah et al., who reported efficiency gains of 5–10% through reflector integration in parabolic trough solar collectors [37]. However, the results of this study surpass those of reflector-aided systems with conventional coatings, highlighting the synergistic effects of Ni-Co coatings and optimized reflector angles. Therefore, this study demonstrates that the combination of Ni-Co coatings with reflectors is a promising pathway for enhancing solar collector efficiency, particularly in regions with high solar insolation.

4.3. Regression Model of Ni-Co Panel

The development of a regression model is a critical step in understanding the relationship between the process variables (flow rate V_0, collector angle θ, and reflector angle α) and the thermal efficiency of a Ni-Co-coated Solar Flat Plate collector (SFPC). The quadratic regression model derived in this study provides a mathematical representation of these interactions, facilitating prediction, optimization, and deeper insight into the factors influencing thermal performance. The model presented in Equation (2) provides a comprehensive framework for exploring the effects of each variable and their interactions on the thermal efficiency of an SFPC system.

$$\begin{aligned} Thermal\ Efficiency\ = -327.325 + 38.352\ V_0 + 7.60783\ \theta + 9.61117\ \alpha - 0.21000\ V_0\theta + \\ 0.1967\ V_0\alpha - 0.01389\ \theta\alpha - 14.8925\ {V_0}^2 - 0.076522\ \theta^2 - 0.103\ \alpha^2 \end{aligned} \quad (2)$$

4.3.1. Analysis of Main Effects

Flow Rate (V_0): The coefficient for V_0 is 38.352, indicating a strong positive influence on thermal efficiency. As the flow rate increased, the thermal efficiency increased, suggesting that higher water flow rates enhanced heat removal from the absorber panel, thus maintaining a more efficient heat transfer process. However, the quadratic term (V_0) has a large negative coefficient (−14.8925), indicating that beyond a certain point, increasing the flow rate reduces the efficiency. This aligns with the findings in the literature [42,43], where excessive flow rates reduced the residence time of water in the collector, leading to insufficient heat absorption. Therefore, there is an optimal flow rate range that maximizes thermal efficiency, emphasizing the importance of careful control in practical applications.
Collector Angle (θ): The coefficient for θ is 7.60783, showing a positive but smaller effect than V_0. This implies that increasing the collector angle moderately enhances the thermal efficiency. The angle of the collector affects the amount of solar radiation captured by the absorber panel, with the optimal angles aligned with the position of the sun for maximum radiation absorption [44,45]. However, the quadratic term θ^2, with a negative coefficient (−0.076522), suggests diminishing returns at larger angles, likely because of the decreased effective exposure to solar radiation as the collector deviates from the optimal tilt.
Reflector Angle (α): The reflector angle α also has a positive effect on the efficiency, with a coefficient of 9.61117. This suggests that increasing the reflector angle can enhance the efficiency by directing more sunlight onto the absorber panel. Reflectors play a key role in concentrating solar radiation, which is particularly beneficial for enhancing the performance of selective coatings such as Ni-Co [46]. The negative quadratic term α^2 (−0.103) indicates that, similar to the flow rate and collector angle, there is an optimal reflector angle beyond which the efficiency gains taper off. This may be due to the fact that overly large angles reduce the effectiveness of the reflector in concentrating sunlight directly onto the absorber.

4.3.2. Interaction Effects

The model also incorporates interaction terms that reveal the combined influence of multiple variables on thermal efficiency. These interactions provide insights into the complex relationships that exist in a solar thermal system, where variables do not act independently but rather influence each other.

Interaction between Flow Rate and Collector Angle ($V_0\theta$): The coefficient for $V_0\theta$ is −0.21000, indicating a slightly negative interaction between the flow rate and collector angle. This suggests that as the flow rate increases, higher collector angles may slightly reduce the efficiency. This could be due to the combined effect of increased flow, which reduces the heat absorption time, and larger collector angles, which may not align optimally

with solar radiation throughout the day. Similarly, many studies [47–50] have observed that increased flow rates may counteract the benefits of certain collector angles, particularly in fixed-angle systems.

Interaction between Flow Rate and Reflector Angle ($V_0\alpha$): The positive coefficient of 0.1967 for $V_0\alpha$ suggests a favorable interaction between the flow rate and reflector angle. This indicates that increasing both the flow rate and reflector angle simultaneously has a compounding positive effect on the thermal efficiency. Higher flow rates paired with larger reflector angles help effectively capture and transfer concentrated solar radiation into the water, thereby maximizing the thermal gain.

Interaction Between Collector Angle and Reflector Angle ($\theta\alpha$): The coefficient for $\theta\alpha$ is -0.01389, indicating a weak negative interaction between the collector angle and reflector angle. This suggests that large reflector angles may slightly diminish the efficiency gains associated with higher collector angles. This can occur if the angle of the reflectors becomes too steep, causing concentrated sunlight to miss the optimal focus on the absorber plate.

4.3.3. Interpretation of the Quadratic Terms

The presence of quadratic terms (V_0^2, θ^2, and α^2) with negative coefficients indicates that each process variable has an optimal point beyond which efficiency is further increased. This finding is crucial for practical applications, as it suggests that there is a balance to be achieved when setting these variables. The quadratic nature of these terms indicates diminishing returns, which are often observed in solar thermal systems [51]. The model emphasizes the need for precise control and optimization of each variable to maintain the efficiency within a desired range.

4.3.4. Implications of the Regression Model

The quadratic regression model offers a predictive tool for optimizing the performance of the Ni-Co-coated SFPC. By inputting different values for V_0, θ, and α, the model can predict the thermal efficiency, allowing system designers to identify configurations that maximize energy capture and thermal performance. The significant coefficients for each variable and their interactions highlight the complexity of the system, in which changes in one parameter can influence the effects of others. Furthermore, the model's structure aligns with previous research that emphasizes the value of response surface methodology in optimizing solar collector performance [52,53]. This model not only provides a means to optimize efficiency, but also helps in understanding the underlying physics of how Ni-Co coatings interact with flow rate, collector orientation, and reflector positioning.

Table 3 presents a comparison between the actual and theoretical thermal efficiency values for the Ni-Co-coated solar panel with reflectors across various configurations of the flow rate, collector angle, and reflector angle. The actual efficiency (η) was measured experimentally, and the theoretical efficiency was calculated using a quadratic regression model. The error, defined as the difference between the actual and theoretical efficiencies, is minimal in most cases, with values generally within the range of $\pm 4\%$. This close alignment between the actual and theoretical efficiencies indicates that the regression model reliably predicts the performance of the Ni-Co panel under different operational conditions [54–56]. The low error rates validate the effectiveness of the model in capturing the influence of key variables on thermal efficiency.

Table 3. Comparison of actual and theoretical efficiency for Ni-Co pane with reflector.

Run Order	The Volume Flow of Water (V_0)	Collector Inclination (θ)	Reflector Inclination (α)	Actual Thermal Efficiency (η)	Theoretical Thermal Efficiency (η)	Error
	L/min	Degree	Degree	%	%	%
1	1.5	45	45	77	77.46	−0.61
2	2.5	45	30	32.6	32.96	−1.10
3	0.5	30	45	53.8	53.58	0.43
4	0.5	45	30	51.7	49.99	3.35
5	1.5	45	45	80.6	83.82	−4.08
6	1.5	45	45	81.1	80.21	1.14
7	2.5	45	60	36.2	35.84	1.01
8	1.5	30	30	37.8	38.52	−1.90
9	0.5	45	60	43.5	42.80	1.68
10	2.5	30	45	45.6	43.78	4.01
11	1.5	45	45	77.1	75.71	1.85
12	1.5	60	60	33.3	34.30	−3.18
13	1.5	45	45	79.5	79.02	0.69
14	1.5	60	30	36.4	34.91	4.10
15	0.5	60	45	54.6	56.02	−2.61
16	1.5	30	60	47.2	45.26	4.15
17	2.5	60	45	33.8	33.50	0.90

4.4. Optimization of Ni-Co Panel

The Ni-Co-coated solar panel with reflectors was optimized using the Box–Behnken design (BBD) methodology to assess the influence of three key variables: water flow rate (V_0), collector inclination (θ), and reflector inclination (α) on thermal efficiency (η). Some research has presented an experimental design and the resulting thermal efficiencies for each run. The BBD approach allows for systematic variation in input parameters, facilitating a robust evaluation of their combined effects on panel efficiency. The obtained thermal efficiency values ranged from a minimum of 32.6% to a maximum of 81.1%, with the highest efficiencies observed at mid-level settings of the flow rate and angles, particularly around the central design points where V_0 = 1.5 L/min, θ = 45°, and α = 45°. This pattern indicates that the optimal performance of the Ni-Co-coated panel was achieved at balanced parameter levels, highlighting the importance of a precise configuration to maximize thermal efficiency. The results underscore the effectiveness of the Box–Behnken design in identifying the optimal operating conditions for solar thermal systems (Table 4).

Table 4. Box–Behnken DOE and responses for Ni-Co panel with reflector.

Run Order	The Volume Flow of Water (V_0)	Collector Inclination (θ)	Reflector Inclination (α)	Thermal Efficiency (η)
	L/min	Degree	Degree	%
1	1.5	45	45	77.0
2	2.5	45	30	32.6
3	0.5	30	45	53.8
4	0.5	45	30	51.7
5	1.5	45	45	80.6
6	1.5	45	45	81.1
7	2.5	45	60	36.2
8	1.5	30	30	37.8

Table 4. *Cont.*

Run Order	The Volume Flow of Water (V_0)	Collector Inclination (θ)	Reflector Inclination (α)	Thermal Efficiency (η)
	L/min	Degree	Degree	%
9	0.5	45	60	43.5
10	2.5	30	45	45.6
11	1.5	45	45	77.1
12	1.5	60	60	33.3
13	1.5	45	45	79.5
14	1.5	60	30	36.4
15	0.5	60	45	54.6
16	1.5	30	60	47.2
17	2.5	60	45	33.8

4.5. Lack of Fit Test

The lack of fit (LF) test is crucial for evaluating the adequacy of the regression model developed to predict the thermal efficiency of a Ni-Co-coated solar panel with reflectors. This test compares the model predictions with the actual experimental data to determine how well the model fits the observed values. LF analysis was conducted for several potential model structures, including linear, two-factor interaction (2FI), quadratic, and cubic models. Given that the ratio between the maximum and minimum responses was 2.45, data transformation was unnecessary, and the actual data could be directly used for fitting. The first step in assessing model fit involved examining the sequential sum of squares (Type I), as shown in Table 5. This Table 5 provides insight into the performance of each model type.

Table 5. Sequential sum of squares (Type I).

Source	Sum of Squares	df	Mean Square	F-Value	*p*-Value Prob > F
Mean vs. Total	47,838	1	47,838		
Linear vs. Mean	470.47	3	156.82	0.4009	0.7547
2FI vs. Linear	113.56	3	37.854	0.0761	0.9715
Quadratic vs. 2FI	4938.8	3	1646.3	351.13	<0.0001
Cubic vs. Quadratic	18.008	3	6.0025	1.621	0.3184
Residual	14.812	4	3.703		
Total	53,394	17	3140.8		

The *p*-values associated with the linear model, two-factor interaction, and cubic model were all greater than 0.05, indicating that these models did not fit the actual data well. In contrast, the quadratic model demonstrated a *p*-value of less than 0.05, suggesting a significant fit with the experimental data. Therefore, the quadratic model was chosen as the most appropriate structure to build the regression model for the Ni-Co panel with reflectors. Further validation was conducted using the LF test statistics presented in Table 6, which reinforces the suitability of the quadratic model.

Table 6. Lack of fit test statistics for Ni-Co panel with reflector.

Source	Sum of Squares	df	Mean Square	F-Value	*p*-Value Prob > F	
Linear	5070.4	9	563.38	152.14	0.0001	
2FI	4956.8	6	826.14	223.1	<0.0001	
Quadratic	18.008	3	6.0025	1.621	0.3184	Suggested
Cubic	0	0				***Aliased***
Pure Error	14.812	4	3.703			

Both the linear and two-factor interaction models exhibited a significant lack of fit ($p < 0.05$), indicating that they were unsuitable for accurately predicting efficiency. The cubic model is aliased, which means that it cannot be used for model building owing to its redundancy with existing terms. However, the quadratic model showed an insignificant lack of fit ($p = 0.3184$), making it the best choice for developing a robust regression model.

4.6. Model Summary Statistics

The model summary statistics, displayed in Table 7, provide additional validation for model selection. These statistics include the standard deviation, R-squared values, adjusted R-squared, predicted R-squared, and prediction error sum of squares (PRESS), which are key indicators of model reliability.

Table 7. Model summary statistics for Ni-Co panel with reflector.

Source	Std. Dev.	R-Squared	Adjusted R-Squared	Predicted R-Squared	PRESS	
Linear	19.778	0.0847	−0.127	−0.326	7367.6	
2FI	22.297	0.1051	−0.432	−1.146	11,920	
Quadratic	**2.1653**	**0.9941**	**0.9865**	**0.944**	**311.26**	**Suggested**
Cubic	1.9243	0.9973	0.9893		+	Aliased

The quadratic model shows a high R-squared value of 0.9941, indicating that 99.41% of the variation in thermal efficiency can be explained by the model. This high R-squared, along with an adjusted R-squared of 0.9865 and predicted R-squared of 0.944, suggests a minimal deviation between the actual and predicted responses. The close alignment between the adjusted and predicted R-squared values further confirms the reliability of the quadratic model, as a difference of less than 0.2 is considered desirable for robust models. Additionally, the PRESS value for the quadratic model (311.26) was significantly lower than that of the linear (7367.6) and two-factor interaction (11,920) models. Lower PRESS values indicate a stronger model fit, reinforcing the conclusion that the quadratic model is best suited to these data.

4.7. Analysis of Variance (ANOVA)

An analysis of variance (ANOVA) was performed on the selected quadratic regression model to assess the statistical significance of each term and interaction in predicting the thermal efficiency of the Ni-Co-coated solar panel with reflectors. ANOVA based on the Type III partial sum of squares was conducted with a 95% confidence level, meaning that the *p*-value threshold for significance was set at 0.05. Any model term or interaction with a *p*-value less than 0.05 is considered to have a significant influence on the thermal efficiency of the response variable.

From Table 8, it is evident that the quadratic model has a significant effect on thermal efficiency. For each individual factor in the model, the water flow rate (V_0), collector inclination (θ), and reflector inclination (α) exhibited statistically significant influences on

the thermal efficiency. This confirms that adjusting these variables has a notable impact on the performance of the Ni-Co-coated panel, aligned with expectations based on solar thermal principles [11,57].

Table 8. Statistics of ANOVA for Ni-Co panel with reflector.

Source	Sum of Squares	df	Mean Square	F-Value	*p*-Value Prob > F	
Model	5522.843	9	613.6492	130.8839	<0.0001	**Significant**
A-Flow Rate (V_0)	383.645	1	383.645	81.82681	<0.0001	
B-Collector Angle (θ)	86.46125	1	86.46125	18.44113	0.0036	
C-Reflector Angle (α)	0.36125	1	0.36125	0.07705	0.0234	
AB	39.69	1	39.69	8.465394	0.0227	
AC	34.81	1	34.81	7.424549	0.0296	
BC	39.0625	1	39.0625	8.331556	0.7328	
A^2	933.8381	1	933.8381	199.1763	<0.0001	
B^2	1248.178	1	1248.178	266.2212	<0.0001	
C^2	2259.929	1	2259.929	482.0153	<0.0001	
Residual	32.8195	7	4.6885			
Lack of Fit	18.0075	3	6.0025	1.620983	0.3184	**not significant**
Pure Error	14.812	4	3.703			
Cor. Total	5555.662	16				

Additionally, the interactions between V_0 and θ and between V_0 and α were significant, indicating that the combined effect of these variables contributed meaningfully to the response. However, the interaction between θ and α did not have a statistically significant influence, as indicated by a *p*-value greater than 0.05. This suggests that the combined effect of the collector and reflector angles on the thermal efficiency is minimal when compared to other interactions, potentially owing to their relatively independent impact on solar radiation absorption and concentration.

The lack of fit (LF) test value for the model was found to be 1.62, which was insignificant. This result implies that the lack of fit is not substantial, indicating that the model fits well with the actual data and that the error is mainly due to pure experimental error rather than a model misfit. This LF value translates to a 31.84% probability of error, which is acceptable for this analysis and further supports the reliability of the model.

4.8. Model Fit and R-Squared Values

Table 9 presents the R-squared values of the quadratic model, which further validate its suitability for predicting thermal efficiency. The adjusted R-squared value of 0.9864 and the predicted R-squared value of 0.9439 were very close to each other, indicating a minimal deviation between the actual and predicted values. This close alignment demonstrates the robustness of the model and confirms its accuracy in predicting the thermal efficiency based on the selected process variables.

Table 9. Values of R-squares for Ni-Co panel with reflector.

Std. Dev.	**2.165294**	**R-Squared**	**0.994093**
Mean	53.04706	**Adj R-Squared**	0.986497
C.V. %	4.081837	**Pred R-Squared**	0.943974
PRESS	311.2638	**Adeq Precision**	28.9922

Moreover, the adequate precision of the model was calculated to be 28.9, which was significantly higher than the threshold value of 4. This high precision indicates a strong signal-to-noise ratio, indicating that the model predictions are reliable and have low noise

interference. A higher adequate precision value suggests that the model predictions were based on well-defined signals, further confirming the accuracy and reliability of the model.

The normal plot of the internally studentized residuals, shown in Figure 6, reveals that the residuals are closely aligned with the reference line and are symmetrically distributed on both sides. This alignment indicated that the residuals were minimal, demonstrating a good fit with the quadratic regression model. This pattern in the residuals is an indication of the model's accuracy in predicting thermal efficiency (Figure 7) without significant bias, further validating its suitability.

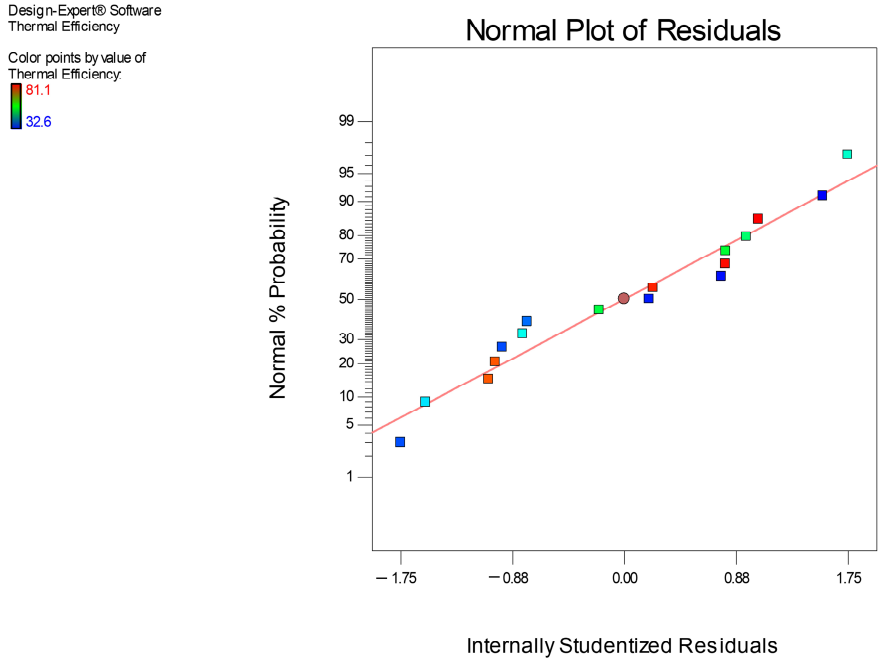


Figure 6. Normal plot of residuals for Ni-Co panel with reflector.

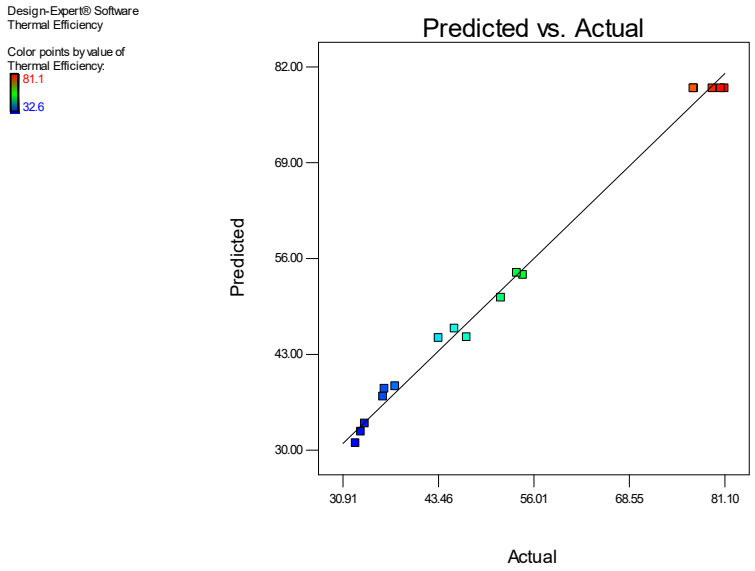


Figure 7. Predicted and actual responses for Ni-Co panel with reflector.

4.9. Surface Plot of the Response

The response contour surface plot in Figure 8 illustrates the combined effects of the water flow rate and collector angle on the thermal efficiency (TE) of the Ni-Co-coated solar flat plate collector (SFPC). As depicted in the plot, TE initially increases with both the

collector angle and flow rate up to optimal levels, beyond which further increases in either parameter result in a decline in efficiency. For the collector angle, the TE improved as the angle increased, reaching a peak efficiency when the angle was optimally aligned with solar incidence. However, as the collector angle exceeds this optimal point, the efficiency starts to decrease, likely owing to misalignment with the incoming solar radiation, which reduces the effectiveness of the absorber in capturing solar energy.

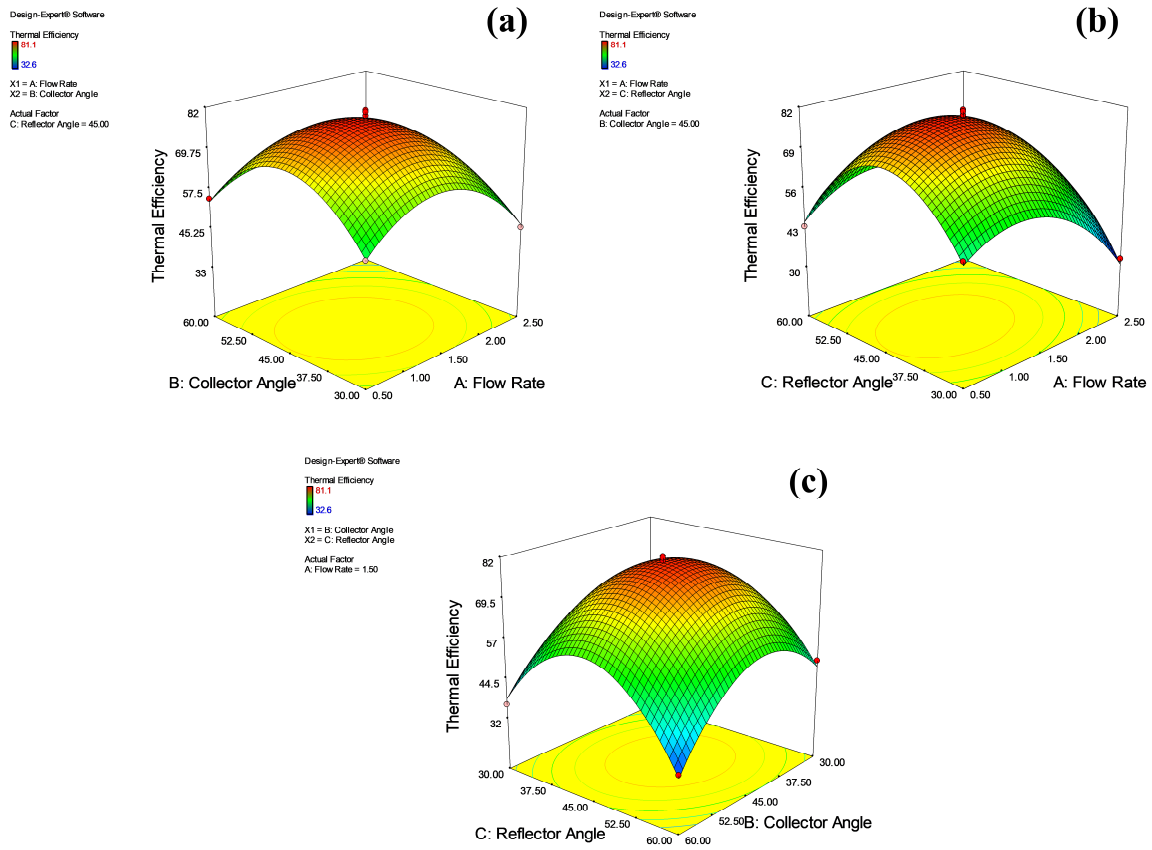


Figure 8. Response surfaces of interactions for nickel-cobalt-coated panel. (**a**) Flow rate vs. collector angle, (**b**) flow rate vs. reflector angle, (**c**) collector angle vs. reflector angle.

Similarly, for the flow rate, an initial increase enhances the TE as it improves the rate of heat transfer within the collector. However, beyond a certain flow rate, the efficiency declines owing to the reduced residence time of water within the absorber, which limits the amount of heat absorbed by the water. This pattern suggests that there are optimal collector angles and flow rates that maximize the thermal efficiency of the SFPC, reinforcing the importance of carefully tuning these parameters to achieve the best performance.

Figure 7 illustrates the distributions of the predicted and actual responses. The close alignment between these two sets of values suggests that the model predictions closely matched the actual data, reinforcing the robustness and reliability of the model in predicting the performance of the Ni-Co-coated panel with reflectors. This consistency between the predicted and observed responses is a strong indicator of the model's practical applicability in optimizing the solar collector efficiency.

An analysis of the effect of the reflector angle on the thermal efficiency (TE) of the Ni-Co-coated solar flat plate collector (SFPC) is shown in Figure 8. The findings reveal that the TE increases with the reflector angle up to a certain point, beyond which the efficiency begins to decline. The maximum efficiency achieved was 81.1% at a reflector angle of 45°, whereas the minimum observed efficiency was 32.6%. The peak efficiency aligns with the optimal angle at which the amount of solar radiation directed to the absorber is maximized.

As the reflector angle increases beyond this optimal point, the efficiency decreases owing to the suboptimal focusing of solar radiation on the absorber surface.

Figure 8 further illustrates the influence of the reflector angle, collector angle, and flow rate on the TE. Variations in TE due to these parameters are explained in the previous sections, emphasizing that each parameter contributes to the collector's overall performance, with optimal settings for each leading to enhanced efficiency. The optimization objective for the performance of the Ni-Co panel in the SFPC is to maximize the TE, subject to the constraints presented in Table 10. Therefore, the collector rate (0.5 to 2.5 L/min), reflector angle (30° to 60°), and reflector angle (30° to 60°), with equal weightage and importance, were assigned to each parameter. Table 11 presents the optimized parameters, where a maximum efficiency of 79.2% was achieved with a flow rate of 1.32 L/min, collector angle of 46.91°, and reflector angle of 42.34°. A desirability score of 0.974 indicates a high degree of accuracy in the optimized results. The predicted maximum efficiency of 79.2% significantly outperforms both uncoated panels (40–50%) [20,29] and panels coated with conventional materials, such as black chrome (60–65%) [16,18]. This highlights the potential of Ni-Co coatings as sustainable and high-performance alternatives capable of achieving efficiency improvements of up to 14% over traditional coatings [39]. Moreover, the integration of reflectors enhanced the overall system performance, contributing an additional 8% efficiency gain [26]. The maximum efficiency of 79.2% achieved in this study has significant implications for real-world solar applications. This efficiency not only enhances energy yield and reduces the carbon footprint, but also lowers operational costs and broadens the applicability of solar collectors across diverse climates. Furthermore, it supports industrial processes requiring high temperatures, such as drying and desalination, and enables integration into hybrid energy systems for improved performance and sustainability.

Table 10. Constraints used for optimizing the performance of Ni-Co panel.

Name	Goal	Lower Limit	Upper Limit	Lower Weight	Upper Weight	Importance
Flow Rate	is in range	0.5	2.5	1	1	3
Collector Angle	is in range	30	60	1	1	3
Reflector Angle	is in range	30	60	1	1	3
Thermal Efficiency	maximize	32.6	81.1	1	1	3

Table 11. Optimized parameters and responses for Ni-Co panel with reflector.

Number	Flow Rate	Collector Angle	Reflector Angle	Thermal Efficiency	Desirability	
1	1.32	46.91	42.34	79.246	0.974	Selected

5. Conclusions

This study evaluated the performance optimization of Ni-Co-coated solar flat plate collectors (SFPCs) for sustainable operation. Key findings include:

- **Efficiency without reflectors:** Ni-Co-coated SFPCs achieved an average thermal efficiency of 50.9%.
- **Efficiency with Reflectors:** Adding reflectors increased the efficiency to an average of 59.0%, demonstrating an 8% improvement.
- **Optimized Parameters:** Using the Box–Behnken design (BBD), the optimal operating conditions were identified as a flow rate of 1.32 L/min, collector angle of 46.91°, and reflector angle of 42.34°, achieving a maximum thermal efficiency of 79.2%.
- **Quantitative Gains:** Reflectors increased incident solar radiation by 36.5 W/m^2 on average and exit water temperature by 7 °C, peaking at 67.3 °C.

- **Predictive Modeling:** A validated quadratic regression model (R^2 = 0.9941) reliably predicted the thermal efficiency based on operational variables.

These results establish Ni-Co-coated panels as a sustainable and efficient alternative to conventional coatings, enhancing solar thermal system performance and supporting broader renewable energy adoption. While this study demonstrates the potential of Ni-Co coatings and reflector-based designs, further research is necessary to explore their long-term durability under various climatic conditions, including extreme temperatures and humidity. Additionally, investigating the integration of advanced materials, such as nanostructured coatings, could provide insights into further improving thermal performance. Future work could also focus on scaling up these systems for industrial applications, examining their economic feasibility, and integrating these collectors into hybrid renewable energy systems. These efforts will contribute to advancing solar thermal technology toward broader adoption and sustainability goals.

Author Contributions: Conceptualization, R.C.; Methodology, R.C. and H.P.; Software, M.A. and P.M.K.; Validation, H.P.; Formal analysis, M.A.; Investigation, H.P.; Writing—original draft, M.A. and P.M.K.; Writing—review & editing, R.C. and H.P.; Supervision, P.M.K. All authors have read and agreed to the published version of the manuscript.

Funding: This research received no external funding.

Institutional Review Board Statement: Not applicable.

Informed Consent Statement: Not applicable.

Data Availability Statement: The data presented in this study are available on request from the corresponding author.

Conflicts of Interest: The authors declare no conflict of interest.

References

1. Vengadesan, E.; Senthil, R. A Review on Recent Developments in Thermal Performance Enhancement Methods of Flat Plate Solar Air Collector. *Renew. Sustain. Energy Rev.* **2020**, *134*, 110315. [CrossRef]
2. Almeshaal, M.; Kumar, P.M. Study on enhancing groundwater quality in a coastal area of Saudi Arabia using a curved glass solar still. *Groundw. Sustain. Dev.* **2024**, *25*, 101154. [CrossRef]
3. Goel, V.; Hans, V.S.; Singh, S.; Kumar, R.; Pathak, S.K.; Singla, M.; Bhattacharyya, S.; Almatrafi, E.; Gill, R.S.; Saini, R.P. A Comprehensive Study on the Progressive Development and Applications of Solar Air Heaters. *Sol. Energy* **2021**, *229*, 112–147. [CrossRef]
4. Hussein, O.A.; Habib, K.; Muhsan, A.S.; Saidur, R.; Alawi, O.A.; Ibrahim, T.K. Thermal Performance Enhancement of a Flat Plate Solar Collector Using Hybrid Nanofluid. *Sol. Energy* **2020**, *204*, 208–222. [CrossRef]
5. Alasiri, A.; Kumar, P.M. Investigating the influence of solar distillation on improving the groundwater quality index in the southern region of Riyadh, Saudi Arabia. *Groundw. Sustain. Dev.* **2024**, *25*, 101155. [CrossRef]
6. Tan, T.; Zhang, H.; Yang, M.; Baeyens, J. Energy-Efficient Crumb Rubber Drying by Heat Recovery and Solar Air Heating. *Ind. Crops Prod.* **2024**, *209*, 117970. [CrossRef]
7. Capossio, J.P.; Fabani, M.P.; Reyes-Urrutia, A.; Torres-Sciancalepore, R.; Deng, Y.; Baeyens, J.; Rodriguez, R.; Mazza, G. Sustainable Solar Drying of Brewer's Spent Grains: A Comparison with Conventional Electric Convective Drying. *Processes* **2022**, *10*, 339. [CrossRef]
8. Michael Joseph Stalin, P.; Rao, P.N.; Palaniappan, M.; Kumar, P.M.; Udhayakumar, K. Effective thermal performance assessment for prismatic triangular solar air heater integrated with fins and turbulators. *Numer. Heat Transf. Part A Appl.* **2024**, 1–17. [CrossRef]
9. Holechek, J.L.; Geli, H.M.E.; Sawalhah, M.N.; Valdez, R. A Global Assessment: Can Renewable Energy Replace Fossil Fuels by 2050? *Sustainability* **2022**, *14*, 4792. [CrossRef]
10. Strielkowski, W.; Civín, L.; Tarkhanova, E.; Tvaronavičienė, M.; Petrenko, Y. Renewable Energy in the Sustainable Development of Electrical Power Sector: A Review. *Energies* **2021**, *14*, 8240. [CrossRef]
11. Sakhaei, S.A.; Valipour, M.S. Performance Enhancement Analysis of The Flat Plate Collectors: A Comprehensive Review. *Renew. Sustain. Energy Rev.* **2019**, *102*, 186–204. [CrossRef]

12. Fudholi, A.; Sopian, K. A Review of Solar Air Flat Plate Collector for Drying Application. *Renew. Sustain. Energy Rev.* **2019**, *102*, 333–345. [CrossRef]
13. Zheng, J.; Febrer, R.; Castro, J.; Kizildag, D.; Rigola, J. A New High-Performance Flat Plate Solar Collector. *Numer. Model. Exp. Validation. Appl. Energy* **2024**, *355*, 122221. [CrossRef]
14. Kumar, P.M.; Mylsamy, K. A comprehensive study on thermal storage characteristics of nano-CeO_2 embedded phase change material and its influence on the performance of evacuated tube solar water heater. *Renew. Energy* **2020**, *162*, 662–676. [CrossRef]
15. Sheikholeslami, M.; Farshad, S.A.; Ebrahimpour, Z.; Said, Z. Recent Progress on Flat Plate Solar Collectors and Photovoltaic Systems in the Presence of Nanofluid: A Review. *J. Clean. Prod.* **2021**, *293*, 126119. [CrossRef]
16. Kumar, P.M.; Kumar, C.S.; Muralidharan, K.; Muniratnam, Y.; Abraham, K.; Manikandan, V.; Stalin, P.M.J.; Prasanth, S.J. Augmenting the performance of conventional solar still through the nano-doped black paint (NDBP) coating on absorber. *Mater. Today: Proc.* **2021**, *47*, 4929–4933. [CrossRef]
17. Chen, M.; Yin, F.; Du, Z.; Sun, Z.; Zou, X.; Bao, X.; Pan, Z.; Tang, J. MOF-derived CuxS double-faced-decorated carbon nanosheets as high-performance and stable counter electrodes for quantum dots solar cells. *J. Colloid. Interface Sci.* **2022**, *628*, 22–30. [CrossRef]
18. Thakur, A.; Kumar, R.; Kumar, S.; Kumar, P. Review of Developments on Flat Plate Solar Collectors for Heat Transfer Enhancements Using Phase Change Materials and Reflectors. *Mater. Today Proc.* **2021**, *45*, 5449–5455. [CrossRef]
19. Verma, S.K.; Sharma, K.; Gupta, N.K.; Soni, P.; Upadhyay, N. "Performance Comparison of Innovative Spiral Shaped Solar Collector Design with Conventional Flat Plate Solar Collector". *Energy* **2020**, *194*, 116853. [CrossRef]
20. Bellos, E.; Tzivanidis, C. Design of a Solar-Driven Cogeneration System Using Flat Plate Collectors and Evacuated Tube Collectors. *Int. J. Energy Res.* **2019**, *43*, 5841–5851. [CrossRef]
21. Alam, T.; Balam, N.B.; Kulkarni, K.S.; Siddiqui, M.I.H.; Kapoor, N.R.; Meena, C.S.; Kumar, A.; Cozzolino, R. Performance Augmentation of the Flat Plate Solar Thermal Collector: A Review. *Energies* **2021**, *14*, 6203. [CrossRef]
22. Sadegh Hosseini, S.M.; Dehaj, M.S. An Experimental Study on Energetic Performance Evaluation of a Parabolic Trough Solar Collector Operating with Al2O3/Water and GO/Water Nanofluids. *Energy* **2021**, *234*, 121317. [CrossRef]
23. Sun, K.; Liu, S.; Gao, Y.; Du, H.; Cheng, D.; Wang, Z. Output power prediction of stratospheric airship solar array based on surrogate model under global wind field. *Chin. J. Aeronaut.* 2024; *in press*. [CrossRef]
24. Prakasam, M.J.S.; Murugesan, P.; Pasupathi, M.K.; Rapuru, L.; Balaji, P.; Murugesan, V. Investigating the Performance of a Flat-plate Solar Water-heating System using CeO_2/Water Nanofluid: A Holistic Approach. *J. Enhanc. Heat Transf.* **2024**, *31*, 47–72. [CrossRef]
25. Hassan, H.; Osman, O.O.; Abdelmoez, M.N.; abo-Elfadl, S. Experimental Assessment of Novel Designed Solar Hot Water Storage Collector Incorporating an Array of Partitioned Ducts Absorber. *Sol. Energy* **2023**, *262*, 111838. [CrossRef]
26. Ramesh, C.; Vijayakumar, M.; Alshahrani, S.; Navaneethakrishnan, G.; Palanisamy, R.; Natrayan, L.; Saleel, C.A.; Afzal, A.; Shaik, S.; Panchal, H. Performance Enhancement of Selective Layer Coated on Solar Absorber Panel with Reflector for Water Heater by Response Surface Method: A Case Study. *Case Stud. Therm. Eng.* **2022**, *36*, 102093. [CrossRef]
27. Pathak, S.K.; Tazmeen, T.; Chopra, K.; Tyagi, V.V.; Anand, S.; Abdulateef, A.M.; Pandey, A.K. Sustainable Energy Progress via Integration of Thermal Energy Storage and Other Performance Enhancement Strategies in FPCs: A Synergistic Review. *Sustainability* **2023**, *15*, 13749. [CrossRef]
28. Wang, H.; Ren, X.; Chen, J.; Xu, W.; He, Q.; Wang, H.; Zhan, F.; Chen, L. Recent Advances of Emerging Oxyhydroxide for Electrochemical Energy Storage Applications. *J. Power Sources* **2023**, *554*, 232309. [CrossRef]
29. Sakhaei, S.A.; Valipour, M.S. Investigation on the Effect of Different Coated Absorber Plates on the Thermal Efficiency of the Flat-Plate Solar Collector. *J. Therm. Anal. Calorim.* **2020**, *140*, 1597–1610. [CrossRef]
30. Qi, J.; Chen, Y.; Li, Q.; Sui, Y.; He, Y.; Meng, Q.; Wei, F.; Ren, Y.; Liu, J. Hierarchical NiCo Layered Double Hydroxide on Reduced Graphene Oxide-Coated Commercial Conductive Textile for Flexible High-Performance Asymmetric Supercapacitors. *J. Power Sources* **2020**, *445*, 227342. [CrossRef]
31. Kumar, M.; Aashish; Negi, B.S.; Shimpy; Grewal, R.; Manchanda, H. Assessment of an ETC Based Solar Water Heater at Different Tilt Angles. *Mater. Today Proc.* 2023, *in press*. [CrossRef]
32. Karmakar, R.; Maji, P.; Ghosh, S.K. A Review on the Nickel Based Metal Matrix Composite Coating. *Met. Mater. Int.* **2021**, *27*, 2134–2145. [CrossRef]
33. Eklund, J.; Phother, J.; Sadeghi, E.; Joshi, S.; Liske, J. High-Temperature Corrosion of HVAF-Sprayed Ni-Based Coatings for Boiler Applications. *Oxid. Met.* **2019**, *91*, 729–747. [CrossRef]
34. Sadeghi, E.; Markocsan, N.; Joshi, S. Advances in Corrosion-Resistant Thermal Spray Coatings for Renewable Energy Power Plants. Part I: Effect of Composition and Microstructure. *J. Therm. Spray Technol.* **2019**, *28*, 1749–1788. [CrossRef]
35. Barwinska, I.; Kopec, M.; Kukla, D.; Senderowski, C.; Kowalewski, Z.L. Thermal Barrier Coatings for High-Temperature Performance of Nickel-Based Superalloys: A Synthetic Review. *Coatings* **2023**, *13*, 769. [CrossRef]
36. Xu, Y.; Hou, M.; Feng, Y.; Li, M.; Yang, S.; Wang, J. Heterogeneous Asymmetric Double-Layer Composite with Ultra-Low Reflection for Electromagnetic Shielding. *Colloids Surf. A Physicochem. Eng. Asp.* **2023**, *669*, 131545. [CrossRef]

37. Ullah, F.; Kang, M. Impact of Air Flow Rate on Drying of Apples and Performance Assessment of Parabolic Trough Solar Collector. *Appl. Therm. Eng.* **2017**, *127*, 275–280. [CrossRef]
38. Ullah, F.; Kang, M. Performance Evaluation of Parabolic Trough Solar Collector with Solar Tracking Tilt Sensor for Water Distillation. *Energy Environ.* **2019**, *30*, 1219–1235. [CrossRef]
39. Kumar, R.; Dixit, A. Corrosion Resists Ni, Co Co-Pigmented Nanoporous Anodized Alumina as Spectral Selective Coating Structure for Solar Thermal Applications. *J. Alloys Compd.* **2019**, *810*, 151833. [CrossRef]
40. Rahimian, M.; Ghaffarinejad, A.; Arabi, M. Water Splitting by Electrodepositing Ni–Co on Graphite Rod: Low-Cost, Durable, and Binder-Free Electrocatalyst. *Int. J. Hydrogen Energy* **2024**, *81*, 852–864. [CrossRef]
41. Faisal Ahmed, S.; Khalid, M.; Vaka, M.; Walvekar, R.; Numan, A.; Khaliq Rasheed, A.; Mujawar Mubarak, N. Recent Progress in Solar Water Heaters and Solar Collectors: A Comprehensive Review. *Therm. Sci. Eng. Prog.* **2021**, *25*, 100981. [CrossRef]
42. Mehari, A.; Xu, Z.Y.; Wang, R.Z. Thermal Energy Storage Using Absorption Cycle and System: A Comprehensive Review. *Energy Convers. Manag.* **2020**, *206*, 112482. [CrossRef]
43. Ahmadi, A.; Ehyaei, M.A.; Doustgani, A.; El Haj Assad, M.; Hmida, A.; Jamali, D.H.; Kumar, R.; Li, Z.X.; Razmjoo, A. Recent Residential Applications of Low-Temperature Solar Collector. *J. Clean. Prod.* **2021**, *279*, 123549. [CrossRef]
44. Vahidhosseini, S.M.; Rashidi, S.; Hsu, S.H.; Yan, W.M.; Rashidi, A. Integration of Solar Thermal Collectors and Heat Pumps with Thermal Energy Storage Systems for Building Energy Demand Reduction: A Comprehensive Review. *J. Energy Storage* **2024**, *95*, 112568. [CrossRef]
45. Hu, J.; Zhang, G. Performance Improvement of Solar Air Collector Based on Airflow Reorganization: A Review. *Appl. Therm. Eng.* **2019**, *155*, 592–611. [CrossRef]
46. Zayed, M.E.; Zhao, J.; Elsheikh, A.H.; Du, Y.; Hammad, F.A.; Ma, L.; Kabeel, A.E.; Sadek, S. Performance Augmentation of Flat Plate Solar Water Collector Using Phase Change Materials and Nanocomposite Phase Change Materials: A Review. *Process Saf. Environ. Prot.* **2019**, *128*, 135–157. [CrossRef]
47. Zhu, Y.; Liu, J.; Yang, X. Design and Performance Analysis of a Solar Tracking System with a Novel Single-Axis Tracking Structure to Maximize Energy Collection. *Appl. Energy* **2020**, *264*, 114647. [CrossRef]
48. Muhumuza, R.; Zacharopoulos, A.; Mondol, J.D.; Smyth, M.; Pugsley, A.; McGee, J. Simulation and Experimental Validation of Solar Radiation Distribution on the Absorber of a Line-Axis Asymmetric Compound Parabolic Concentrator. *Sol. Energy* **2020**, *198*, 36–52. [CrossRef]
49. Wang, H.; Huang, J.; Song, M.; Yan, J. Effects of Receiver Parameters on the Optical Performance of a Fixed-Focus Fresnel Lens Solar Concentrator/Cavity Receiver System in Solar Cooker. *Appl. Energy* **2019**, *237*, 70–82. [CrossRef]
50. Manikandan, G.K.; Iniyan, S.; Goic, R. Enhancing the Optical and Thermal Efficiency of a Parabolic Trough Collector—A Review. *Appl. Energy* **2019**, *235*, 1524–1540. [CrossRef]
51. Battisti, F.G.; de Araujo Passos, L.A.; da Silva, A.K. Performance Mapping of Packed-Bed Thermal Energy Storage Systems for Concentrating Solar-Powered Plants Using Supercritical Carbon Dioxide. *Appl. Therm. Eng.* **2021**, *183*, 116032. [CrossRef]
52. Gil, J.D.; Topa, A.; Álvarez, J.D.; Torres, J.L.; Pérez, M. A Review from Design to Control of Solar Systems for Supplying Heat in Industrial Process Applications. *Renew. Sustain. Energy Rev.* **2022**, *163*, 112461. [CrossRef]
53. Gautam, A.; Saini, R.P. A Review on Sensible Heat Based Packed Bed Solar Thermal Energy Storage System for Low Temperature Applications. *Sol. Energy* **2020**, *207*, 937–956. [CrossRef]
54. Farouk, W.M.; Hamisa, G.; Omara, Z.M.; Essa, F.A. Mathematical Modeling and Optimization of Pyramidal Still Performance Using Response Surface Method and Ag-Nanoparticle Enhanced Phase Change Material. *J. Energy Storage* **2024**, *75*, 109569. [CrossRef]
55. Shaban, W.M.; Kabeel, A.E.; El Hadi Attia, M.; Talaat, F.M. Optimizing Photovoltaic Thermal Solar Systems Efficiency through Advanced Artificial Intelligence Driven Thermal Management Techniques. *Appl. Therm. Eng.* **2024**, *247*, 123029. [CrossRef]
56. Li, Z.; Yu, X.; Wang, L.; Lu, Y.; Huang, R.; Chang, J.; Jiang, R. Effects of Fluctuating Thermal Sources on a Shell-and-Tube Latent Thermal Energy Storage during Charging Process. *Energy* **2020**, *199*, 117400. [CrossRef]
57. Azha, N.I.S.; Hussin, H.; Nasif, M.S.; Hussain, T. Thermal Performance Enhancement in Flat Plate Solar Collector Solar Water Heater: A Review. *Processes* **2020**, *8*, 756. [CrossRef]

Disclaimer/Publisher's Note: The statements, opinions and data contained in all publications are solely those of the individual author(s) and contributor(s) and not of MDPI and/or the editor(s). MDPI and/or the editor(s) disclaim responsibility for any injury to people or property resulting from any ideas, methods, instructions or products referred to in the content.